Optical property of an antireflection coating fabricated by an optimal spin-coating method with a pH-modified SiO_2 nanoparticle solution

Chyan-Chyi Wu (吳乾埼)[1], Cheng-Chih Hsu (許正治)[2,*], Yu-Chian Lin (林宇謙)[2], Chia-Wei Chiang (江家維)[2], and Ching-Lian Dai (戴慶良)[3]

[1]*Department of Mechanical and Electromechanical Engineering, Tamkang University, New Taipei City 25137, China*
[2]*Department of Photonics Engineering, Yuan Ze University, 135, Yuan-Tung Road, Chung-Li 32003, China*
[3]*Department of Mechanical Engineering, Taiwan Chung Hsing University, Taichung 402, China*
**Corresponding author: cchsu@saturn.yzu.edu.tw*

Received September 15, 2016; accepted December 2, 2016; posted online December 30, 2016

An antireflection (AR) coating is fabricated by applying an optimal spin-coating method and a pH-modified SiO_2 nanoparticle solution on a cover glass. Because the pH value of the solution will affect the aggregation and dispersion of the SiO_2 particles, the transmittance of the AR-treated cover glass will be enhanced under optimal fabricated conditions. The experimental results show that an AR coating fabricated by an SiO_2 nanoparticle solution of pH 11 enhances the transmittance approximately by 3% and 5% under normal and oblique incident conditions, respectively. Furthermore, the AR-treated cover glass exhibits hydrophobicity and shows a 65% enhancement at a contact angle to bare glass.

OCIS codes: 310.1210, 160.4236, 310.5448, 220.4241.
doi: 10.3788/COL201715.023101.

Antireflection (AR) coatings are widely used in optical elements and electronic devices, such as mirrors, prisms, planar displays, and solar cell modules. Especially in planar displays and solar cell modules, the power consumption is a crucial factor in these devices, and energy can be preserved by enhancing the received power or emitted intensity of such devices. The idea behind AR coatings can be realized by depositing a single/multiple dielectric thin film with a suitable refractive index on a substrate[1–3]. This kind of AR coating can be classified as a homogeneous AR coating[4,5]. Unfortunately, the transmittance enhancement of this kind of AR coating is limited to a single wavelength, a narrow wavelength bandwidth, or to a normal incidence of light. In this case, a gradient refractive index (gradient-RI) AR coating, also called an inhomogeneous AR coating[4,5], becomes a desirable method for improving the transmittance. Different profiles of the gradient-RI AR coating have been proposed, and there are a number of different fabrication methods of gradient-RI AR coatings, including roller imprinting/nanoimprinting surface texturing[6–8], spin coating[7,9,10], chemical deposition[11], and the self-assembled method[10,12]. Krebs[7] and Yao[10] reviewed the current literature regarding the fabrication process of AR coatings for solar cells. They also highlighted the advantages and drawbacks of the existing methods. In spite of the complexity of AR-coating formation, spin coating and roller imprinting allow for a highly reproducible formation over a large area. In an earlier study[9], we proposed a two-step spin-on-glass (SOG) method to fabricate AR coatings with SiO_2 nanospheres and showed that the transmittance of the AR coating decreased as its water absorption increased.

This work successfully demonstrates the AR-treated cover glass fabricated by spinning a pH-modified SiO_2 nanoparticle solution on a cover glass with an optimal spin-coating method. The pH modification of the SiO_2 nanoparticle solution can change the aggregation and dispersion of the SiO_2 particles. It also affects the surface energy of AR coatings fabricated by pH-modified SiO_2 nanoparticles. Therefore, the transmittance and hydrophobicity of the AR-treated cover glass can be enhanced under optimal fabrication conditions. The SiO_2 nanosphere AR coating is prepared using the optimal spin-coating method, as shown in Fig. 1. As disclosed in our previous work[9], many critical factors affect the transmittance of SiO_2 nanospheres AR coatings, such as the size of the SiO_2 nanospheres, the rotation speed, the rotation time, and the baking temperature. These critical fabricated parameters are indicated in Fig. 1.

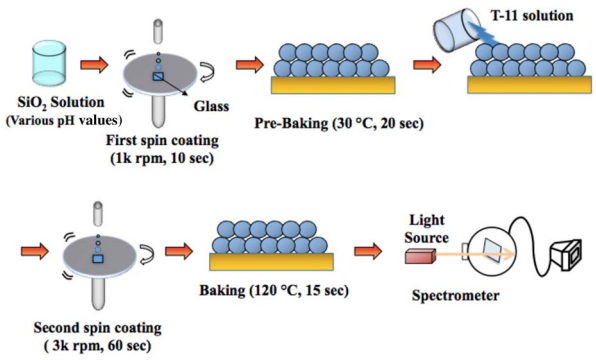

Fig. 1. Diagram of optimal spin-coating method.

In this study, a tempered glass substrate is cleaned using an ultrasonic cleaner in absolute ethanol for 5 min and then dried with an N_2 air gun. Then, it is covered with 0.3 mL of an SiO_2 nanoparticle solution, and the first step of the SOG procedure begins. The pre-baking follows the first step of the SOG procedure. The disposed sample is then covered with 0.3 mL of Honeywell Accuglass® T-11, and the second step of the SOG procedure starts. After that, the sample is kept first at 70°C for 10 s for solvent removal and then at 120°C for 15 s for cross-linking in the SOG film.

The SiO_2 nanosphere solution is obtained from a commercial chemical company (Nissan Chemical Industries Ltd). The average size of the SiO_2 nanospheres and the pH value of the suspension are approximately 100 nm and 9, respectively. To demonstrate the pH dependence of the nanoparticle size and the corresponding transmittance enhancement of the AR coating fabricated with such a material, the pH value of the suspension was controlled in terms of alkalinity and acid by adding the appropriate amounts of hydrochloric acid and sodium hydroxide. The particle sizes of various pH values of the suspension were determined by a dynamic laser scattering (DLS) method, as shown in Fig. 2(a). Obviously, the alkaline suspension induced the aggregation of the SiO_2 particles and increased the particle size distribution from 100 to 150 nm. In contrast with the alkaline suspension, the acidic suspension generated the dispersion behaviors of SiO_2 particle and increased the particle size distribution from 100 to 70 nm[13–15]. Figure 2(b) shows the transmittance measurements of the AR coating with various pH values of the SiO_2 nanoparticle solution. The results indicated that the transmittance of the AR coating fabricated by the acidic suspension of SiO_2 nanoparticles exhibited poor enhancement compared to the AR coating fabricated by the alkaline suspension of SiO_2 nanoparticles. Additionally, the transmittance behaviors of the suspensions of SiO_2 nanoparticles with pH values of 3 and 5 were worse than the result of bare glass. Therefore, the pH value of the suspension of SiO_2 nanoparticles was controlled at 6, 9, and 11 to demonstrate the optical property of the AR coating.

Figure 2(c) shows the top-view SEM image of the AR coating fabricated by various pH values of SiO_2 solutions. The sizes of the nanoparticle shown in Fig. 2(c) are 65, 99, and 138 nm for the various pH values of the suspension. It is obvious that the structure exhibited a more compact and high filling factor as the particle size distribution became narrower. Therefore, a more porous structure will be located inside the noncompact structure, leading to the lower effective refractive and achieved high transparency[16,17].

To demonstrate the transparency of the AR coating fabricated by various pH values of SiO_2 nanoparticle solutions under different incident angles, the transmittance variation and power ratio within the wavelength range of 400–900 nm are shown in Fig. 3. Figures 3(a)–3(c) show the transmittance variation within the wavelength range of 400–900 nm and the incident angles controlled at 0°,

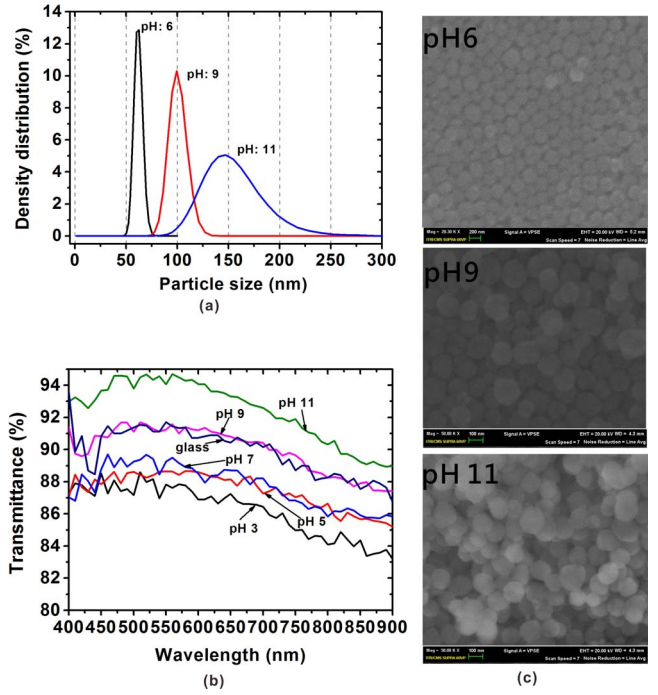

Fig. 2. Properties of various pH values of SiO_2 nanoparticle solution. (a) Particle distribution of various pH values of SiO_2 nanoparticle solution measured by the DLS. (b) Transmittance of the AR coating fabricated with various pH values of the SiO_2 solution. (c) Top-view SEM image of AR coating fabricated by various pH values of SiO_2 solution.

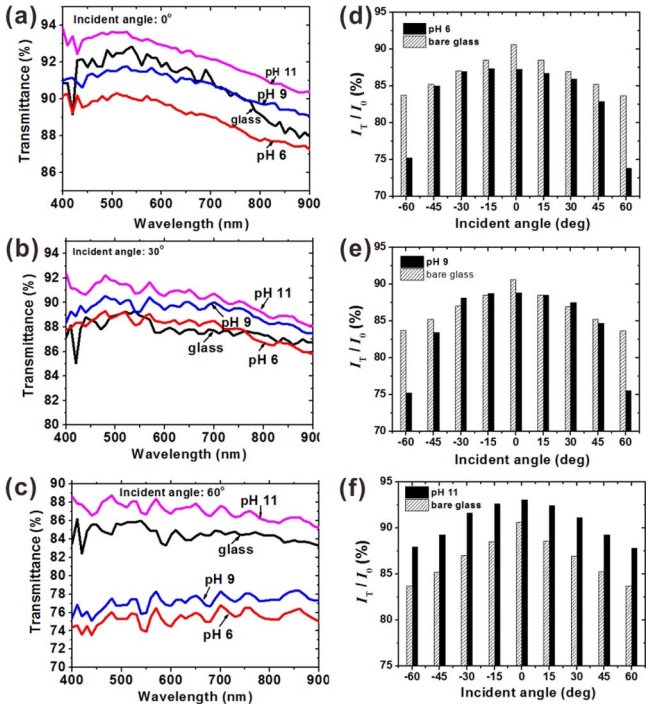

Fig. 3. Transparency of the AR coating with various pH values of SiO_2 solution under different incident angles. (a)–(c) Transmittance variation within the wavelength range from 400–900 nm. (d)–(f) Power ratio within an incident angle range of ±60°.

30°, and 60°. Obviously, the optimum transmittance enhancement can be obtained by the AR coating fabricated by the SiO_2 nanoparticle solution with the pH value of 11. The results also showed that the transmittance of the AR coating (pH 11) can be preserved by more than 86% with a wide incident angle.

In order to evaluate the transmitted power within the wavelength range from 400–900 nm and at various incident angles (−60°–60°), the power ratios are calculated and shown in Figs. 3(d)–3(f). The power ratio is defined as the ratio of the transmitted intensity (I_T) to the initial intensity (I_0) in which the intensity (I_T) can be estimated by the area under the transmittance: the wavelength curve. Obviously, the power ratio of the AR coating fabricated by the SiO_2 nanoparticle solution with the pH value of 11 produced a larger enhancement than those results of bare glass under various incident angles.

Figures 4 and 5 show the transmittance variation and power ratio of the AR coating with polarized light incident at various angles. In Fig. 4(a), the transmittance variations of p- and s-polarized light remained at similar levels under normal incident conditions for the AR coatings fabricated by the SiO_2 nanoparticle solutions at various pH values. As the incident angle increased [incident angles of 30° and 60° in Figs. 4(b) and 4(c), respectively], the transmittance variations of the p- and s-polarized light of the AR coating were no longer similar. The results show that the transmittance of p-polarized light was preserved by 90%; in contrast, the transmittance of s-polarized light decreased as the incident angle increased. Figure 5 indicates the power ratio of the various pH values of the fabricated AR coatings that were incident by p- and s-polarized light under different incident angles within the range of ±60°.

The power ratios of the p-polarized light of the AR coating fabricated by various pH values of SiO_2 nanoparticle solutions were greater than 90%. The power ratio of the

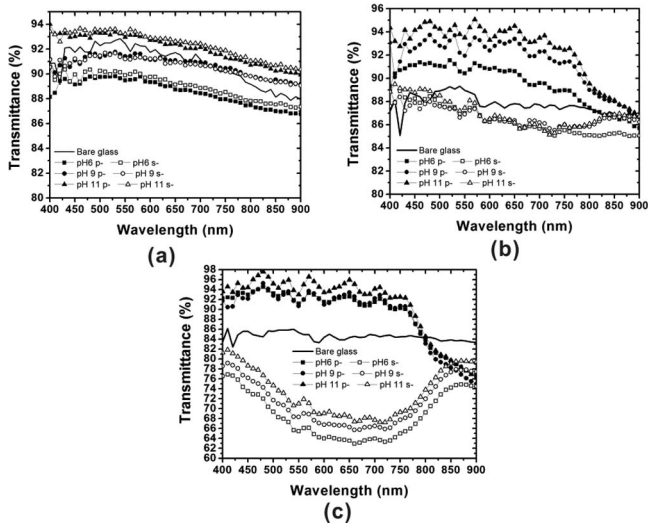

Fig. 4. Transparency of the AR coating with various pH values of SiO_2 solution under different incident angles with p- and s-polarized light. (a) 0°, (b) 30°, and (c) 60°.

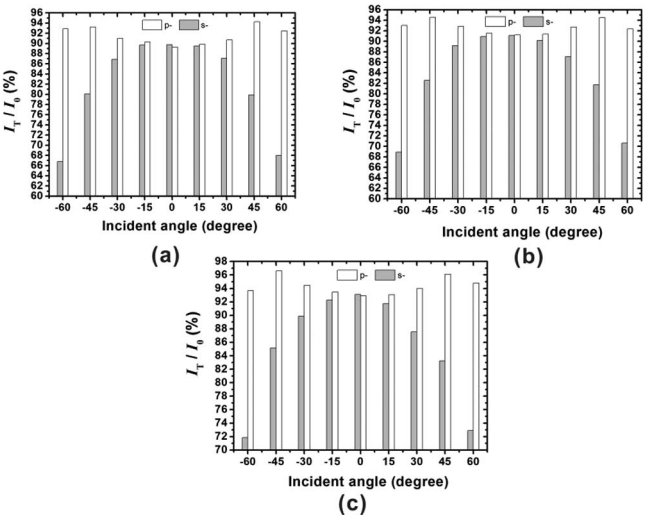

Fig. 5. Power ratio of the AR coating with various pH values of SiO_2 solution under different incident angles with p-and s-polarized light measured within an incident angle range of ±60°. (a) pH 6, (b) pH 9, and (c) pH 11.

s-polarized light of those AR coatings decreased as the incident angle increased. The power ratio decreases from the normal incident condition to the oblique incident condition (±60°) were 26%, 25%, and 22% for the AR coating fabricated by the SiO_2 nanoparticle solution with pH values of 6, 9, and 11, respectively. Additionally, the ratio decreased sharply at the incident angles between 45°–60° and −45°– − 60°. Based on these findings, the transmittance exhibited was high relative to the polarization property of the incident light. These results were followed the transmittance behavior of the thin film structure, which can be simulated with Airy's formulas[18].

Furthermore, the Brewster's angles of each AR coating fabricated by various pH values of SiO_2 nanoparticle solutions can be obtained by measuring the reflectance variation; they are shown in Fig. 6(a). The Brewster's angles of each AR coating fabricated by the SiO_2 solutions with pH value of 11 and 6 were approximated of 50° and 55°, respectively.

Based on the Brewster's angle condition[18],

$$\tan \theta_B = \frac{n_{\text{effective RI}}}{n_{\text{air}}}. \tag{1}$$

The effective refractive index ($n_{\text{effective RI}}$) of the cover glass with the AR coating can be calculated, and the values of $n_{\text{effective RI}}$ were approximately 1.15 and 1.25. A theoretical simulation of the Brewster's angles of various effective refractive indices ($n_{\text{effective RI}}$) is shown in Fig. 6(b).

The theoretical simulation indicated that the Brewster's angle increased as the effective refractive index increased because the effective refractive of the AR coating depended on the filling factor of the SiO_2 particle. The AR coating fabricated with a large-sized SiO_2 particle exhibited a small filling factor and indicated that more air filled the unit volume. Therefore, the effective refractive index

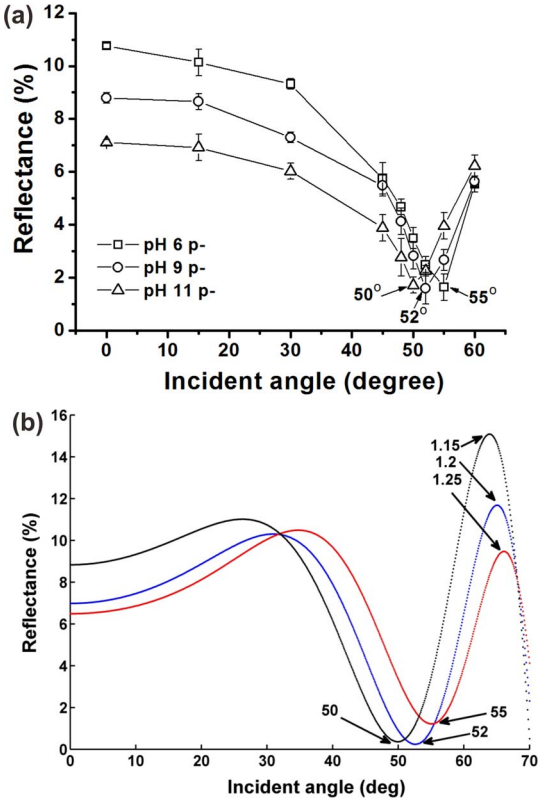

Fig. 6. Reflectance of the AR coating with various pH values of the SiO_2 solution under p-polarized light. (a) Experimental results. (b) Theoretical simulation.

will be smaller than those AR coatings fabricated by small-sized SiO_2 particles. The larger size of the SiO_2 particle we used, the smaller the effective refractive index of the fabricated AR coating. The particle size of the SiO_2 solution with the pH value of 11 is larger than the solution with the pH of 6. The AR coating fabricated by the solution with the pH value of 11 exhibited a smaller filling factor, in which the effective refractive index of the AR coating will be smaller than the AR coating fabricated by the solution with the pH value of 6.

Figure 7 shows the contact angle measurements of the AR coatings fabricated with various pH values. The AR coatings fabricated with pH values of 6 and 9 exhibited hydrophilic surfaces. By contrast, the AR coating fabricated with the pH value of 11 exhibited a hydrophobic surface. The largest contact angle can be observed at approximately 99°, which was 20% higher than the AR coating fabricated by the SiO_2 solution with the pH value of 6. Compared to the contact angle of the water-glass interface (approximately 35°[19]), the enhancement was higher than 65%.

The mechanism of the enhancement of the contact angle is complicated. Based on the roughness-induced hydrophobicity, the hierarchical roughness structure of the AR coating fabricated by the SiO_2 solution with the pH value of 11 demonstrated high-enough asperities to resist the capillary wave and prevented nanodroplets from filling in the valleys between asperities[20]. Additionally, the pH

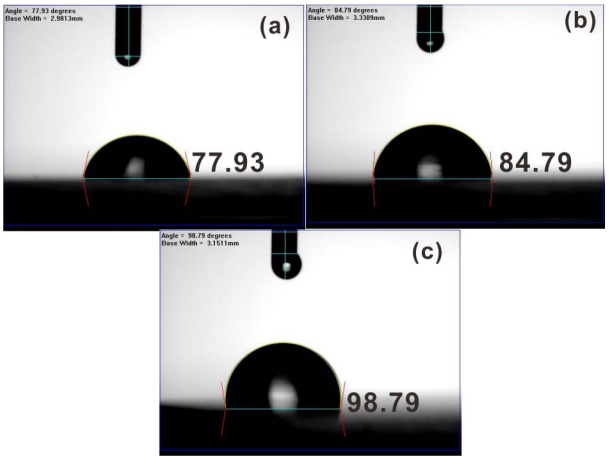

Fig. 7. Hydrophobic nature of the AR coating with various pH values of SiO_2 solution. (a) pH 6, (b) pH 9, and (c) pH 11.

modification of the SiO_2 solution also affected the surface energy between the AR coating (fabricated by the SiO_2 nanoparticle) and water. Based on van Oss's[21] study, the acidic treatment of the glass surface exhibited as hydrophilic, and the alkaline treatment of the glass exhibited as hydrophobic. Therefore, we believe that the hydrophobic enhancement resulted from the hierarchical roughness structure and the surface energy changes of the AR coating fabricated by the pH-modified SiO_2 nanoparticle.

This work demonstrates AR coatings fabricated by a pH-modified SiO_2 nanoparticle solution with the optimum spin-coating method on a cover glass. Because the properties of aggregation, dispersion, and surface energy by the pH-modified SiO_2 nanoparticle solution will be modified, the transparence, polarization dependence, and hydrophobicity of the cover glass will be affected. The results show that the optimum transmittance of the AR coating can be obtained by fabricating it with a solution of pH 11, resulting in an enhancement of 3% to bare glass under the normal incident condition. The results show that the power ratio of the s-polarized light decreases as the incident angle increases. By contrast, the power ratio of the p-polarized light increases as the incident angle increases. Furthermore, the effective refractive index of the AR coating can be obtained by applying Brewster's angle condition, and an effective refractive index of 1.25 can be reached by the AR coating fabricated by the SiO_2 nanoparticle solution of pH 11. Finally, the AR coating provided the hydrophobicity, and the contact angle can be enhanced to 65% higher than bare glass. Based on these findings, we can conclude that the proposed method has some advantages, such as an easy and low-cost fabrication procedure, acceptable optical transmittance within a wide range of incident angles and wavelengths, and a self-cleaning hydrophobic surface.

The authors would like to thank the National Science Council of China for financially supporting this research under Contract No. NSC 102-2221-E-155-076-MY3. The authors also thank Ted Kony for his editorial assistance.

References

1. H. A. Macleod, *Thin Film Optical Filters*, 3rd ed. (Taylor & Francis, 2001).
2. S. J. Liu and W. A. Chen, Opt. Laser Technol. **48**, 226 (2013).
3. N. Wang, Y. Zhu, W. Wei, J. Chen, P. Li, and Y. Wen, Opt. Commun. **284**, 4773 (2011).
4. J. A. Dobrowolski, "Optical properties of films and coatings," in *Handbook of Optics*, M. Bass, ed. (McGraw-Hill, 1995).
5. J. A. Dobrowolski, D. Poitras, P. Ma, H. Vakil, and M. Acree, Appl. Opt. **41**, 3075 (2002).
6. K. Suzuki, S. Youn, Q. Wang, H. Hiroshima, and Y. Nishioka, Jpn. J. Appl. Phys. **52**, 06GJ06 (2013).
7. F. C. Krebs, Sol. Eng. Mat. Sol. Cells **93**, 394 (2009).
8. M. Tao, W. Zhou, H. Yang, and L. Chen, Appl. Phys. Lett. **91**, 081118 (2007).
9. C. C. Hsu, W. L. Lan, N. P. Chen, and C. C. Wu, Opt. Laser Technol. **58**, 202 (2014).
10. L. Yao and J. He, Prog. Mater. Sci. **61**, 94 (2014).
11. T. Minemoto, T. Mizuta, H. Takakura, and Y. Hamakawa, Sol. Energ. Mat. Sol. Cells **91**, 191 (2007).
12. Y. Zhao, J. Wang, and G. Mao, Opt. Lett. **30**, 1885 (2005).
13. R. K. Iler, *The Chemistry of Silica* (John Wiley & Sons, 1979).
14. T. Graham, J. Chem. Soc. **17**, 318 (1864).
15. X. Wang, Z. Shen, T. Sang, X. Cheng, M. Li, L. Chen, and Z. Wang, J. Colloid Interface Sci. **341**, 23 (2010).
16. A. Gombert, W. Glaubitt, K. Rose, J. Dreibholz, and B. Blasi, Solar Energy **68**, 357 (2000).
17. M. J. Minot, J. Opt. Soc. Am. **66**, 515 (1976).
18. P. Yeh, *Optical Waves in Layered Media* (John Wiley & Sons, 1991).
19. W. Wu and G. H. Nancollas, Adv. Dent. Res. **11**, 566 (1997).
20. M. Nosonovsky and B. Bhushan, Microelectron. Eng. **84**, 86–382 (2007).
21. C. J. van Oss, *Interfacial Force in Aqueous Media* (Dekker, 1994).